J. Chem. Eng. Data 1988, 33, 111–115

Boiling points of the binary system were correlated by the equation suggested by Wisniak and Tamir (*7*):

$$T = x_1T_1 + x_2T_2 + x_1x_2[C_0 + C_1(x_1 - x_2) + C_2(x_1 - x_2)^2 + \dots] \quad (5)$$

An optimization technique yielded the following values for the constants: $C_0 = -51.325$, $C_1 = 29.786$, $C_2 = 22.484$, $C_3 = 60.637$, $C_4 = 134.786$, with a coefficient of determination of 0.970.

Acknowledgment

Yehudit Reizner and Moshe Golden helped in the experimental and numerical calculations.

Glossary

α, β, δ	constants
B_{ii}, B_{ij}	virial coefficient
P	overall pressure, mmHg
P_i^0	vapor pressure of pure component, mmHg
R	gas constant
t, T	temperature, °C, K
v_i^L	molar volume of pure liquid *i*, mL/mol
x_i, y_i	molar fraction of component *i* in the liquid and vapor phases
γ_i	activity coefficient of component *i*

Subscripts

i, j, k	component *i*, *j*, *k*

Registry No. Methanol, 67-56-1; 1,1-dichloroethane, 75-34-3.

Literature Cited

(1) Boublikova, L.; Lu, B. C. Y. *J. Appl. Chem.* **1969**, *19*, 89.
(2) Wisniak, J.; Tamir, A. *J. Chem. Eng. Data* **1975**, *20*, 168.
(3) TRC Tables; *Selected Values of Properties of Chemical Compounds*; Thermodynamic Research Center Data Project: College Station, TX, 1974.
(4) Tsonopoulos, C. *AIChE J.* **1974**, *20*, 263.
(5) Tsonopoulos, C. *AIChE J.* **1975**, *21*, 827.
(6) Redlich, O.; Kister, A. T. *Ind. Eng. Chem.* **1948**, *40*, 345.
(7) Wisniak, J.; Tamir, A. *Chem. Eng. Sci.* **1975**, *30*, 335.

Received for review July 15, 1987. Accepted January 4, 1988.

Vapor–Liquid Equilibria for the Ethane–Propane System at Low Temperature

Claude J. Blanc* and Jean-Claude B. Setier
Groupement de Recherches de Lacq, LNG Laboratory, Elf-Aquitaine, B.P. 34, Lacq, 64170 Artix, France

Vapor–liquid equilibrium data for the ethane–propane mixture at 270, 255.4, 245, 235, 210, and 195 K are reported. These data have been correlated with good accuracy by the Soave, Redlich–Kwong, and Peng–Robinson equations of state, allowing a variation with temperature of the binary interaction parameter. Variation of equimolar excess Gibbs energy with temperature is also reported.

Introduction

This experimental study is a part of an extensive research program on natural gas liquefaction and cryogenic treatments. Accurate data on ethane–propane equilibria at low temperature are necessary in several fields: prediction of the behavior of mixed refrigerant cycles in gas liquefaction units; heavy hydrocarbon removal from natural gas to be liquefied; ethane extraction from natural gas for ethylene production.

The data obtained complement those published by Djordjevich and Budenholzer (*1*) who performed 47 equilibria determinations at various temperatures with a large internal between there (25 K). Hirata et al. (*2*) and Skripka et al. (*3*) have also published some equilibrium values at low temperature.

Equipment and Experiment

The closed-loop vapor recirculation apparatus is of the type described by Kidnay et al. (*4*). The equilibrium cell and close surroundings are shown in Figure 1. The external and internal diameters of the equilibrium cell, realized in sapphire, are respectively 6.5 and 4.5 cm; the height is 9.5 cm. Available volume for liquid and vapor phases is about 140 cm^3. This original apparatus has been manufactured by Société des Matériels Cryogéniques (SMC) based on laboratory specifications.

Temperature is measured by platinum resistance thermometers at four different locations in the equilibrium cell. They are calibrated every 2 months with pure methane. Vapor pressure versus temperature data used are those published by the National Bureau of Standards (*5*, *6*). Accuracy is within 0.015 K. Pressure is measured by a Mensor-QM quartz gauge accurate to 0.5 kPa for a 5 MPa pressure value.

All samples are analyzed by gas chromatography using a 2.2-m column packed with 60/80 mesh silica gel at 120 °C. For the vapor phase, a cylindrical container mounted on the recirculation system is used. When equilibrium is reached, this container is isolated and then connected to chromatograph through valves. For the liquid, a sample less than 0.1 cm^3 is taken from the bulk, using a 0.02 cm diameter capillary tube, and entirely vaporized into an exhausted container where it is homogenized by a magnetically driven turbine.

Chromatographic peaks are then processed by a Hewlett-Packard 3354 integrating computer. The gases used were supplied by L'Air Liquide. The purity was 99.95%. Further purification has been applied to propane by flowing it through dried 5A molecular sieve.

Results and Discussion

The unsmoothed 152 data obtained at seven different temperatures ranging from 270 to 195 K are reported in Tables I–VII. In addition to the pressure and mole fractions *X* and *Y* of the lighter constituent in liquid and vapor phases, respectively, the *K* values of the two components are also reported.

0021-9568/88/1733-0111$01.50/0

Table I. Experimental P–x–y Equilibrium Data for the C_2H_6–C_3H_8 System at 270 K[a]

P, MPa	$X(C_2H_6)$	$Y(C_2H_6)$	$K(C_2H_6)$	$K(C_3H_8)$
0.4960	0.0469	0.1864	3.9744	0.8536
0.5058	0.0493	0.1997	4.0507	0.8418
0.5308	0.0720	0.2575	3.5764	0.8001
0.5361	0.0760	0.2690	3.5395	0.7911
0.5470	0.0831	0.2903	3.4934	0.7740
0.6335	0.1422	0.4281	3.0105	0.6667
0.6477	0.1519	0.4413	2.9052	0.6588
0.6588	0.1567	0.4529	2.8902	0.6488
0.7191	0.2001	0.5218	2.6077	0.5978
0.7348	0.2098	0.5391	2.5696	0.5833
0.7509	0.2203	0.5542	2.5157	0.5718
0.8343	0.2740	0.6103	2.2274	0.5368
0.8544	0.2878	0.6281	2.1824	0.5222
0.8750	0.2996	0.6409	2.1392	0.5127
1.0921	0.4331	0.7508	1.7335	0.4396
1.1193	0.4497	0.7620	1.6945	0.4325
1.1506	0.4623	0.7724	1.6708	0.4233
1.4356	0.6288	0.8611	1.3694	0.3742
1.4673	0.6437	0.8674	1.3475	0.3722
1.4895	0.6469	0.8733	1.3500	0.3588
1.9169	0.8686	0.9551	1.0996	0.3417
1.9380	0.8801	0.9590	1.0896	0.3420
1.9720	0.8957	0.9653	1.0777	0.3327

[a] P_0 (C_2H_6) = 2.2033 MPa; P_0 (C_3H_8) = 0.4295 MPa.

Table II. Experimental P–x–y Equilibrium Data for the C_2H_6–C_3H_8 System at 255.4 K[a]

P, MPa	$X(C_2H_6)$	$Y(C_2H_6)$	$K(C_2H_6)$	$K(C_3H_8)$
0.3634	0.0953	0.3380	3.5467	0.7317
0.3637	0.0946	0.3389	3.5825	0.7302
0.4282	0.1534	0.4648	3.0300	0.6322
0.4289	0.1536	0.4670	3.0404	0.6297
0.5197	0.2376	0.5986	2.5194	0.5265
0.5210	0.2371	0.6015	2.5369	0.5223
0.5797	0.2923	0.6589	2.2542	0.4820
0.5807	0.2929	0.6604	2.2547	0.4803
0.5821	0.2916	0.6593	2.2610	0.4809
0.6669	0.3672	0.7279	1.9823	0.4300
0.6679	0.3675	0.7299	1.9861	0.4270
0.6712	0.3692	0.7294	1.9756	0.4290
0.7649	0.4494	0.7876	1.7526	0.3858
0.7664	0.4491	0.7878	1.7542	0.3852
0.7822	0.4643	0.7985	1.7198	0.3761
0.7945	0.4760	0.8048	1.6908	0.3725
0.9330	0.5871	0.8613	1.4670	0.3359
0.9387	0.5921	0.8632	1.4579	0.3354
0.9927	0.6325	0.8814	1.3935	0.3227
0.9942	0.6339	0.8839	1.3944	0.3171
1.0060	0.6376	0.8846	1.3874	0.3184
1.1112	0.7246	0.9167	1.2651	0.3025
1.1165	0.7283	0.9175	1.2598	0.3036
1.1188	0.7283	0.9173	1.2595	0.3044
1.2079	0.7955	0.9405	1.1823	0.2910
1.2082	0.7982	0.9415	1.1795	0.2899
1.2123	0.7983	0.9406	1.1783	0.2945
1.3206	0.8780	0.9642	1.0982	0.2934
1.3226	0.8782	0.9634	1.0970	0.3005

[a] P_0 (C_2H_6) = 1.5061 MPa; P_0 (C_3H_8) = 0.2612 MPa.

Finally, the experimental pressure value P_0 of each component, measured in the cryostat, is indicated for each temperature.

Correlation of these data has been made in the first step, using the Redlich–Kwong equation of state as modified by Soave (*7*)

$$P = \frac{RT}{v - b} - \frac{a(T)}{v(v + b)}$$

and the Peng–Robinson equation of state (*8*)

$$P = \frac{RT}{v - b} - \frac{a(T)}{v(v + b) + b(v - b)}$$

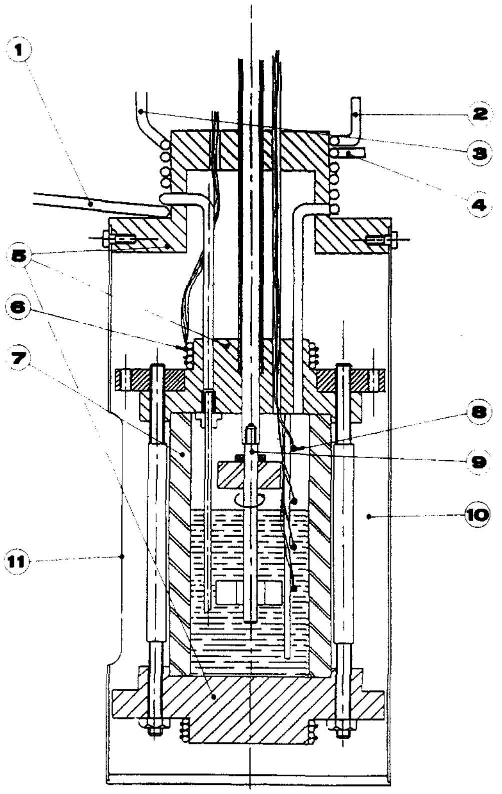

Figure 1. Schematic diagram of the cryostat: (1) inlet liquid nitrogen; (2) outlet gaseous nitrogen; (3) inlet fluid process; (4) outlet fluid process; (5) heat exchanger; (6) electrical resistance (connected to a temperature regulator); (7) sapphire equilibrium cell; (8) platinum resistance thermometer; (9) magnetic stirrer; (10) vacuum; (11) glass window.

Table III. Experimental P–x–y Equilibrium Data for the C_2H_6–C_3H_8 System at 245 K[a]

P, MPa	$X(C_2H_6)$	$Y(C_2H_6)$	$K(C_2H_6)$	$K(C_3H_8)$
0.2320	0.0633	0.3072	4.8531	0.7396
0.2337	0.0647	0.3194	4.9366	0.7277
0.2358	0.0667	0.3255	4.8801	0.7227
0.2548	0.0917	0.3640	3.9695	0.7002
0.2581	0.0955	0.3559	3.7267	0.7121
0.2624	0.1004	0.4216	4.1992	0.6430
0.2648	0.1031	0.4350	4.2192	0.6299
0.3395	0.1939	0.5796	2.9892	0.5215
0.3461	0.2027	0.5925	2.9230	0.5111
0.3510	0.2041	0.5996	2.9378	0.5031
0.4394	0.3079	0.7206	2.3404	0.4037
0.4475	0.3167	0.7226	2.2817	0.4060
0.4538	0.3178	0.7309	2.2999	0.3945
0.5370	0.4202	0.8016	1.9077	0.3422
0.5466	0.4280	0.8060	1.8832	0.3392
0.5535	0.4303	0.8115	1.8859	0.3309
0.6548	0.5435	0.8663	1.5939	0.2929
0.6616	0.5497	0.8706	1.5838	0.2874
0.6678	0.5519	0.8709	1.5780	0.2881
0.9292	0.8299	0.9564	1.1524	0.2563
0.9324	0.8330	0.9564	1.1481	0.2611
0.9349	0.8339	0.9563	1.1468	0.2631
0.9722	0.8756	0.9668	1.1042	0.2669
0.9725	0.8733	0.9664	1.1066	0.2652
0.9730	0.8774	0.9674	1.1026	0.2659
1.0032	0.9014	0.9749	1.0815	0.2546
1.0077	0.9059	0.9762	1.0776	0.2529
1.0114	0.9084	0.9767	1.0752	0.2544

[a] P_0 (C_2H_6) = 1.1221 MPa; P_0 (C_3H_8) = 0.1820 MPa.

The mixing rules used are those defined by these authors, that is

$$a = \sum_i \sum_j x_i x_j a_{ij}$$

Table IV. Experimental P-x-y Equilibrium Data for the C_2H_6-C_3H_8 System at 235 K[a]

P, MPa	$X(C_2H_6)$	$Y(C_2H_6)$	$K(C_2H_6)$	$K(C_3H_8)$
0.2045	0.1277	0.4911	3.8457	0.5834
0.2059	0.1296	0.4974	3.8380	0.5774
0.2819	0.2512	0.6783	2.7002	0.4296
0.2821	0.2517	0.6747	2.6806	0.4347
0.3988	0.4393	0.8493	1.9333	0.2688
0.4032	0.4367	0.8511	1.9489	0.2643
0.4866	0.5647	0.8857	1.5684	0.2626
0.4867	0.5677	0.8867	1.5619	0.2621
0.5102	0.5989	0.9060	1.5128	0.2344
0.5148	0.6007	0.9058	1.5079	0.2359
0.5158	0.6045	0.9083	1.5026	0.2319
0.5782	0.6964	0.9257	1.3293	0.2447
0.5797	0.6952	0.9253	1.3310	0.2451
0.6152	0.7494	0.9383	1.2521	0.2462
0.6181	0.7544	0.9401	1.2462	0.2439
0.6196	0.7551	0.9399	1.2447	0.2454
0.7138	0.8882	0.9735	1.0960	0.2370
0.7229	0.8867	0.9740	1.0985	0.2295

[a] P_0 (C_2H_6) = 0.8239 MPa; P_0 (C_3H_8) = 0.1199 MPa.

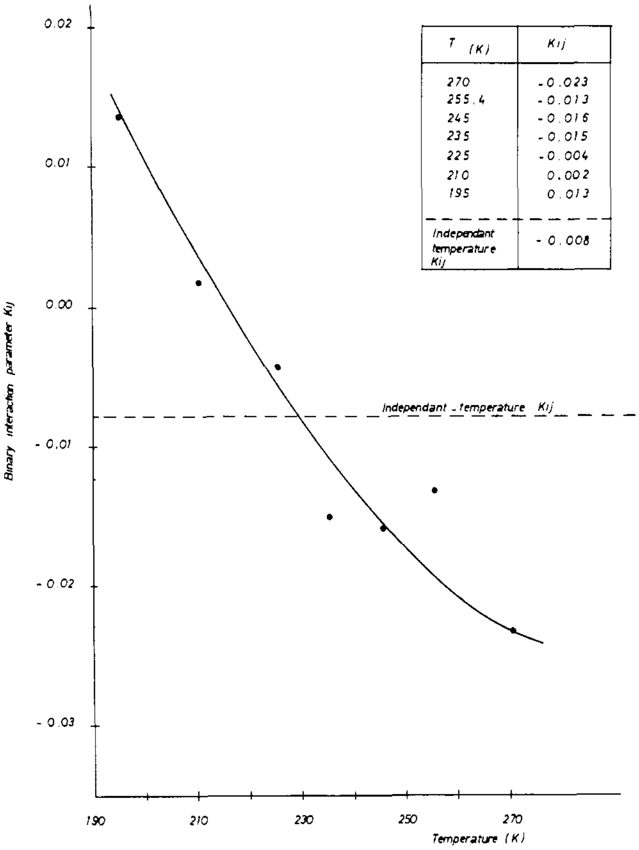

T (K)	Kij
270	-0.023
255.4	-0.013
245	-0.016
235	-0.015
225	-0.004
210	0.002
195	0.013
Independant temperature Kij	- 0.008

Figure 2. Binary interaction parameter K_{ij} versus temperature (Soave–Redlich–Kwong equation of state).

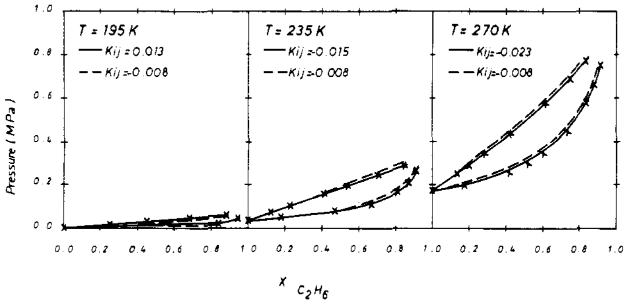

Figure 3. Comparison of experimental data and Soave–Redlich–Kwong equation of state predictions with both single temperature-independent and temperature-dependent binary interaction parameters.

Table V. Experimental P-x-y Equilibrium Data for the C_2H_6-C_3H_8 System at 225 K

P, MPa	$X(C_2H_6)$	$Y(C_2H_6)$	$K(C_2H_6)$	$K(C_3H_8)$
0.0782	0.0006	0.0045	7.5000	0.9961
0.0993	0.0440	0.2730	6.2045	0.7605
0.1001	0.0447	0.2799	6.2617	0.7538
0.1218	0.0906	0.4404	4.8609	0.6154
0.1227	0.0936	0.4501	4.8088	0.6067
0.1239	0.0950	0.4623	4.8663	0.5941
0.1911	0.2305	0.6865	2.9783	0.4074
0.1928	0.2357	0.6882	2.9198	0.4080
0.2130	0.2844	0.7370	2.5914	0.3675
0.2216	0.2943	0.7694	2.6143	0.3268
0.2235	0.2969	0.7704	2.5948	0.3266
0.2334	0.3305	0.7871	2.3815	0.3180
0.2786	0.4294	0.8394	1.9548	0.2815
0.2799	0.4213	0.8439	2.0031	0.2697
0.3351	0.5339	0.8908	1.6685	0.2343
0.3363	0.5314	0.8920	1.6786	0.2305
0.3586	0.5752	0.9096	1.5814	0.2128
0.3600	0.5762	0.9055	1.5715	0.2230
0.4688	0.7766	0.9590	1.2349	0.1835
0.4703	0.7822	0.9613	1.2290	0.1777

[a] P_0 (C_2H_6) = 0.5945 MPa; P_0 (C_3H_8) = 0.0760 MPa.

Table VI. Experimental P-x-y Equilibrium Data fo the C_2H_6-C_3H_8 System at 210 K[a]

P, MPa	$X(C_2H_6)$	$Y(C_2H_6)$	$K(C_2H_6)$	$K(C_3H_8)$
0.0514	0.0581	0.3316	5.7074	0.7096
0.0533	0.0490	0.3316	6.7673	0.7028
0.0666	0.1031	0.5312	5.1523	0.5227
0.0669	0.1100	0.5378	4.8891	0.5193
0.0891	0.1797	0.6883	3.8303	0.3800
0.0898	0.1763	0.6946	3.9399	0.3708
0.1278	0.3151	0.8262	2.6220	0.2538
0.1287	0.3165	0.8209	2.5937	0.2620
0.1290	0.3128	0.8225	2.6295	0.2583
0.1665	0.4433	0.8911	2.0102	0.1956
0.1668	0.4406	0.8892	2.0182	0.1981
0.2156	0.6129	0.9349	1.5254	0.1682
0.2159	0.6150	0.9348	1.5200	0.1694
0.2374	0.6985	0.9477	1.3568	0.1735
0.2425	0.7010	0.9541	1.3611	0.1535
0.2781	0.8353	0.9733	1.1652	0.1621
0.2828	0.8357	0.9758	1.1676	0.1473
0.2866	0.8550	0.9768	1.1425	0.1600

[a] P_0 (C_2H_6) = 0.3338 MPa; P_0 (C_3H_8) = 0.0363 MPa.

Table VII. Experimental P-x-y Equilibrium Data for the C_2H_6-C_3H_8 System at 195 K[a]

P, MPa	$X(C_2H_6)$	$Y(C_2H_6)$	$K(C_2H_6)$	$K(C_3H_8)$
0.0302	0.0764	0.4636	6.0681	0.5808
0.0304	0.0749	0.4638	6.1923	0.5796
0.0503	0.2213	0.7631	3.4483	0.3042
0.0504	0.2242	0.7611	3.3947	0.3079
0.0706	0.3573	0.8611	2.4100	0.2161
0.0871	0.4683	0.9097	1.9426	0.1698
0.0874	0.4707	0.9101	1.9335	0.1698
0.1053	0.5547	0.9318	1.6798	0.1532
0.1055	0.5580	0.9315	1.6694	0.1550
0.1061	0.5677	0.9276	1.6340	0.1675
0.1241	0.6667	0.9537	1.4305	0.1389
0.1283	0.7077	0.9621	1.3595	0.1297
0.1285	0.7041	0.9614	1.3654	0.1304
0.1578	0.9206	0.9874	1.0726	0.1587
0.1583	0.9157	0.9873	1.0782	0.1507

[a] P_0 (C_2H_6) = 0.1757 MPa; P_0 (C_3H_8) = 0.0147 MPa.

Table VIII. Values of Constants Used in the Equations of State

	T_c, K	P_c, MPa	w
ethane	305.33	4.871	0.099
propane	369.85	4.247	0.152

with

$$a_{ij} = (a_i a_j)^{0.5}(1 - K_{ij})$$

$$b = \sum_i X b_i$$

Values of the constants used for calculation of a_i and b_i parameters of the two equations of state, i.e., critical temperature T_c and pressure P_c and Pitzer acentric factor w, are given in Table VIII.

The binary interaction parameter K_{ij} has been determined by an optimization procedure in order to get the minimum deviation between experimental compositions of liquid and vapor phase and those predicted by the equation of state. The binary interaction parameter K_{ij} is obtained by minimizing the function f:

$$f = \sum_i (X_{C_2H_6}{}^{calcd} - X_{C_2H_6}{}^{exptl})^2 + (Y_{C_2H_6}{}^{calcd} - Y_{C_2H_6}{}^{exptl})^2$$

Two procedures were used to effect this minimization. In the first case, the binary interaction parameter K_{ij} is considered as possibly temperature dependent. The function f is thus minimized by using only the data corresponding to the same temperature values. The second procedure consists in determining one independent-temperature binary interaction parameter from all the data obtained.

Figure 2 shows the various values obtained by using, for example, the Soave–Redlich–Kwong equation of state. Binary interaction parameter is observed to decrease sharply as temperature increased. The experimental values and the calculated ones from this equation of state with both temperature-dependent and temperature-independent K_{ij} are shown in Figure 3, for three different temperatures.

Figure 4 shows the deviation of the mole fractions of the experimental ethane vapor phase from those calculated from this equation of state under the same temperature conditions as those of Figure 3.

As appears from these figures, the difference between measured and calculated values is generally small and model-based results are closer to the experimental one when a temperature-dependent binary interaction parameter is used. The sum of the squared differences between calculated and experimental X and Y for the 152 values obtained is 0.08 when the interaction parameter is temperature dependent and 0.12 when it has a constant value. Results obtained by using the Peng–Robinson equation of state are very close to those derived from the Soave equation. The sums of the squared differences between calculated and measured values of mole fractions are 0.06 and 0.09, respectively, according as the binary parameter K_{ij} varies or not with temperature.

Another method to correlate the VLE data obtained is to derive excess Gibbs energy G^E as a function of temperature and composition. The composition dependance of G^E is obtained from

$$G^E = x_1 RT \ln \gamma_1 + x_2 RT \ln \gamma_2$$

where γ_1 and γ_2 are the activity coefficients. These coefficients are obtained from the liquid-phase data by the Barker method (*9*). Virial coefficients needed by this method are taken from Dymond et al. (*10*). Figure 5 gives the variation of equimolar excess Gibbs energy G^E as a function of the temperature. This figure shows that G^E is decreasing continuously as temperature increases.

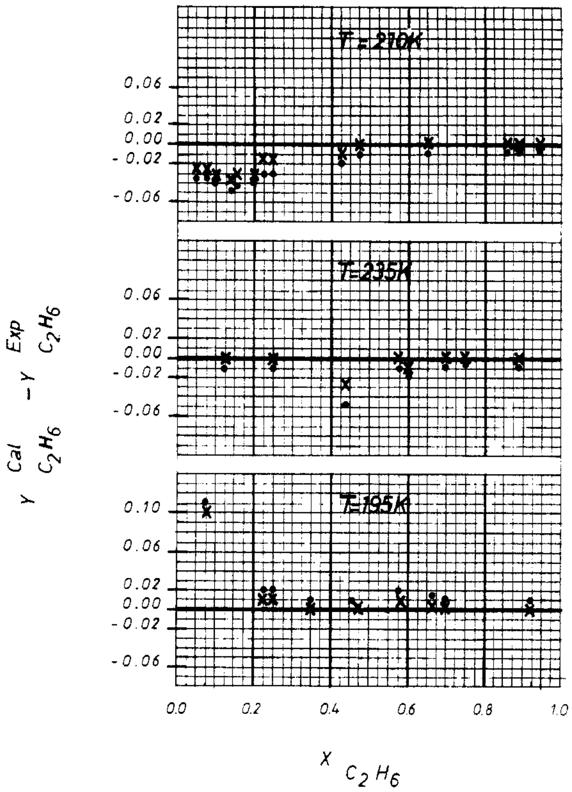

Figure 4. Deviations between experimental vapor-phase mole fractions and those calculated with the Soave equation of state by using a temperature-dependent (X) and a temperature-independant binary interaction parameter (•) for the ethane–propane system at three different temperatures.

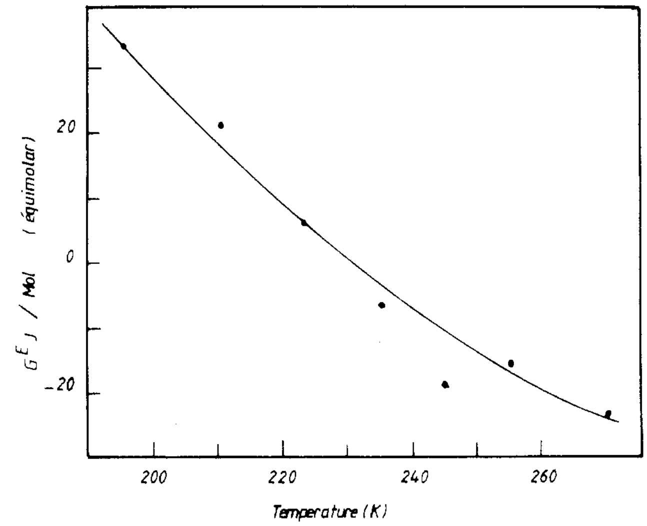

Figure 5. Equimolar excess Gibbs energy versus temperature.

Glossary

a, b	equation of state constants
G^E	excess Gibbs energy
γ	activity coefficient
K_{ij}	binary interaction parameter
P	pressure
R	ideal gas constant
T	temperature
V	molecular volume
X	liquid-phase mole fraction
Y	vapor-phase mole fraction
w	Pitzer acentric factor

Acknowledgment

We express our gratitude to Veronique Munoz for her assistance in the laboratory, and to Philippe Meline and and Claude Leibovici for their aid in computer programs.

Registry No. Ethane, 74-84-0; propane, 74-98-6.

Literature Cited

(1) Djordjevich, L.; Budenholzer, R. A. *J. Chem. Eng. Data* **1970**, *15*, 10.
(2) Hirata, M.; Suda, T.; Hakuta, H.; Nagahama, H. *Mem. Fac. Technol. Tokyo Metrop. Univ.* **1969**, *19*, 103.
(3) Skripka, V.; Nikita, I.; Shadanovich, L. *Gazov. Promst.* **1970**, *15*, 35.
(4) Kidnay, A.; Miller, R.; Parrish, N.; Hiza, M. *Cryogenics* **1975**, Sept. 531.
(5) Prydz, R.; Goodwin, R.; Goodwin, J. *J. Chem. Thermodyn.* **1972**, *4*, 127.
(6) Goodwin, R. *NBS Tech. Note (U.S.)* **1974**, No. 653.
(7) Soave, G. *Chem. Eng. Sci.* **1972**, *27*, 1197.
(8) Peng, D.; Robinson, D. *Ind. Eng. Chem. Fundam.* **1976**, *15*, 59.
(9) Barker, J. *Aust. J. Chem.* **1953**, *6*, 207.
(10) Dymond, J.; Smith, E. *The virial coefficients of gases. A critical compilation*; Clarendon: Oxford, UK, 1969.

Received for review January 2, 1987. Revised September 28, 1987. Accepted October 23, 1987.

PVT of Toluene at Temperatures to 673 K

G. C. Straty,* M. J. Ball, and T. J. Bruno

Thermophysics Division, National Engineering Laboratory, National Bureau of Standards, Boulder, Colorado 80303

Measurements of the *PVT* behavior of compressed gaseous and liquid toluene are reported. Pressure versus temperature observations were made along paths of very nearly constant density (pseudoisochores) in the temperature range from about 348 to over 673 K and at pressures to about 35 MPa. Twenty-seven pseudoisochores were determined ranging in density from about 1.7 to near 9 mol/dm^3.

Introduction

Measurements of the *PVT* behavior of compressed toluene are reported for the temperature range from about 348 to over 673 K at pressures to about 35 MPa. Pressure versus temperature observations were made along paths of nearly constant density (pseudoisochores). Twenty-seven pseudoisochores were determined ranging in density from 1.7 to about 9 mol/dm^3.

Experiment

The reagent grade toluene used in this study was analyzed by gas chromatography. Small quantities (less than 0.07%) of benzene, ethylbenzene, and thiophene were found to be present. Purification with sulfuric acid, followed by distillation, reduced the impurity level to less than 0.001%. The major remaining impurity was benzene which was present at this low level regardless of the lot of starting material.

Measurements were made using an automated high-temperature *PVT* apparatus, which has been described in detail (*1*). Measurements were made by confining the toluene samples in a thick-walled, very nearly constant volume, stainless steel cell and measuring the pressure as a function of temperature to define the locus of *PT* points along paths of very nearly constant density. Cell temperatures were determined with a platinum resistance thermometer calibrated, with respect to the IPTS-1968, by the National Bureau of Standards. Pressures were determined from the frequency of a commercial vibrating quartz pressure transducer calibrated frequently against a primary dead weight gauge and are estimated accurate to the greater of 10 kPa or 0.05%. At the completion of a series of *PT* observations (a run) the toluene samples were condensed into a detachable cylinder, held at liquid nitrogen temperature, for subsequent weighing to determine the number of moles of sample in the system during the measurements. Densities assigned to each *PT* point were then calculated from the calibrated volumes of the system. Small corrections were made for thermal expansion and pressure dilation of the cell and for the small quantities of fluid residing in the various noxious volumes.

Table I. Decomposition Products Detected in Toluene[a]

compound	mol %
dimethylbiphenyl	15.0
stilbene	5.7
diphenylmethane	4.8
methylbiphenyl	4.8
benzene	1.4
benzyltoluene	1.3
dibenzyl	0.5
biphenyl	0.1
fluorene	0.1
anthracene	0.1
pnenathrene	0.1
unidentified components	0.1
toluene	balance

[a] Toluene at 723 K, 15 MPa, for 48 h.

Results and Discussion

The maximum temperature for the initial run reached 723 K; however, decomposition and reaction of the toluene became severe at the highest temperature, as was evidenced by an unacceptable increase in the measured pressure with time. Measurements on a sample at a density of approximately 4 mol/dm^3, held at a temperature of 723 K for 24 h, exhibited a pressure rise of over 20 kPa/h and showed no signs of approaching equilibrium. Results of an analysis of a sample of toluene held for 48 h at 723 K and a pressure of 15 MPa are shown in Table I. Chemical denaturation of the toluene was found to increase appreciably at temperatures above 643 K with ethylbenzene being the main reaction product. An upper limit of 673 K was set for the *PVT* measurements, however, since the pressure increase with time at this temperature was found to be sufficiently small (0.6 kPa/h for the 4 mol/dm^3 test sample) and the residence time for the sample at temperatures over 643 K was normally less than about 8 h. The resulting pressure error due to toluene reaction is probably less than 6.0 kPa and is within the normal uncertainty in the pressure measurements. After each run, the contents of the *PVT* cell were analyzed by gas chromatography and found to be essentially identical with the starting samples.